Facial selectivity in 1,3-dipolar cycloadditions to *cis*-3,4-dimethylcyclobutene. An experimental and computational study

Mauro Freccero,*[a] Remo Gandolfi,[a] Mirko Sarzi-Amadè[a] and Augusto Rastelli[b]

[a] *Dipartimento di Chimica Organica, Università di Pavia, V.le Taramelli 10, 27100 Pavia, Italy*
[b] *Dipartimento di Chimica, Università di Modena, Via Campi 183, 41100 Modena, Italy*

Received (in Cambridge) 10th July 1998, Accepted 3rd September 1998

Facial selectivity in 1,3-dipolar cycloaddition of diazomethane (**2a**), 3,4-dihydroisoquinoline *N*-oxide (**2b**), pyrroline *N*-oxide (**2c**), 5,5-dimethylpyrroline *N*-oxide (**2d**) and several nitrile oxides (**2e**–**2j**) with *cis*-3,4-dimethylcyclobutene (**1**) has been investigated. The stereochemistry of the cycloaddition of **2a**, **2b**–**2d** and encumbered nitrile oxides (**2i** and **2j**) is controlled by steric interactions with dominant formation of the *anti* diastereoisomer. *Syn* and *anti* attack compete with each other in the cases of phenylglyoxylonitrile oxide and pyruvonitrile oxide (**2g** and **2h**, respectively) thus disclosing the presence of contrasteric electronic *syn* orienting effects. Transition state structures of the cycloaddition of formonitrile oxide, diazomethane and methyleneamine *N*-oxide (nitrone) were located with both HF/6-31G* and B3LYP/6-31G* methods. The calculated relative free enthalpies of these transition states satisfactorily reproduce, at both levels, the observed facial selectivity while geometry data suggest a higher steric demand for the nitrone with respect to the other two dipoles. To the best of our knowledge this is the first study of diastereofacial selectivity in 1,3-dipolar cycloaddition with DFT theory.

Introduction

1,3-Dipolar cycloadditions on *cis*-3,4-disubstituted cyclobutenes have been extensively investigated, with both experimental[1–6] and theoretical[1,7–11] approaches. The reason for such interest is due to the systematic parallelism of the diastereoselectivity of these reactions (measured by product distribution analysis) with the pyramidalization of the olefinic carbons. Such a property can be conveniently measured by the out-of-plane bending of the olefinic hydrogens, as was clearly shown by a systematic optimization of the substrate geometry by *ab initio* calculations.[1,7–11] Electron withdrawing substituents on the cyclobutene ring (such as Cl and OR groups) give rise to dominant *syn* addition by 1,3-dipoles (*e.g.*, >96% with diazomethane), whereas small carbocyclic substituents (as in bicyclo[2.1.0]pent-2-ene or bicyclo[2.2.0]hex-2-ene) lead to >93% *anti* addition.[1,7]

Ab initio calculations performed on cyclobutenes with electron withdrawing *cis*-3,4-substituents showed a *syn* pyramidalization, owing to an *anti* (with respect to the substituents) out-of-plane bending of the olefinic hydrogens (*e.g.*, $\alpha = -3.0°$ and $-3.9°$ at the HF/6-31G* and B3LYP/6-31G* levels, respectively, for dichlorocyclobutene).[11] The opposite is true for the substrates, with small carbocyclic substituents, with a strong *anti* pyramidalization which results from a *syn* out-of-plane bending of the olefinic hydrogens higher than $+4°$.[1,7,10]

On the basis of extensive computational work we rationalized the *syn* (or *anti*) pyramidalization as a consequence of the tendency in these systems to maximize the hyperconjugative delocalization between the σ allylic bonds and the π bond. This stereoelectronic stabilizing interaction is even more operative at the transition state (TS) (as a delocalization between σ allylic bonds and forming bonds) and it strongly contributes to the control of the face selectivity of these reactions.[1,7–11] In this context the lack of data about facial selectivity of the reaction of *cis*-3,4-disubstituted cyclobutenes bearing acyclic alkyl groups, the only ones with a weak electron donating character, was disturbing and led us to study the reactivity of *cis*-3,4-dimethylcyclobutene in 1,3-dipolar cycloadditions.

Previous *ab initio* calculations on *cis*-3,4-dimethylcyclobutene (**1**) showed a slightly *syn* pyramidalisation of the olefinic carbons, with a bending angle of the olefinic hydrogens of $-0.9°$ (HF/4-31G).[1] The ground state non planarity of the double bond suggests that there should be a related energy asymmetry of the out-of-plane bending of the olefinic hydrogens on going towards the TS, where the olefinic carbons are more pyramidalized. In fact when a fixed deformation of the olefinic hydrogens of $+20°$ (*syn*) and $-20°$ (*anti*) was imposed on **1** the resulting *syn* bent form (*anti* pyramidalized) was found to be slightly less stable ($E_{+20°} - E_{-20°} = 2.9$ kJ mol^{-1}) than the *anti* bent form.[1] In other words the same weak electronic interaction that causes the *syn* pyramidalization of the substrate could favor the *syn* addition to **1**.

With the aim of shedding further light on the role of steric and stereoelectronic effects of the methyl groups in determining facial selectivity, we decided to investigate the distribution of the *syn* and *anti* adducts in cycloadditions of **1** with 1,3-dipoles (**2**), and to calculate the transition structures of the reactions of the cyclobutene **1** with diazomethane (CH_2N_2, **2a**), formonitrile oxide (HCNO) and methyleneamine *N*-oxide [$H_2C{=}N(O)H$, nitrone], respectively, by *ab initio* methods both at the HF/6-31G* level and with introduction of electron correlation at the B3LYP/6-31G* level.

It was also of interest to compare facial selectivity for the reactions of **1** to that, already studied by us, of *cis*-3,4-dimethyl-1-methoxycarbonylcyclobutene,[12] in order to precisely define the role of the presence of an electron withdrawing substituent on the double bond when facial selectivity is controlled by alkyl groups.

cis-3,4-Dimethylcyclobutene was prepared as described by Brauman[13] starting from a photochemical [2 + 2] sensitized cycloaddition of acetylene with maleic anhydride, with a four step synthesis, modifying the final one according to reference 14.

Experimental

Results

The reactions of cyclobutene **1** (Scheme 1) were carried out at room temperature in the presence of a slight excess of 1,3-dipole, in order to obtain high conversions of the dipolarophile.

The reaction with diazomethane (**2a**) was performed in ethyl ether while those with nitrones (**2b**–**2d**) and nitrile oxides (**2e**–**2j**), were carried out in benzene. Nitrile oxides were generated *in situ* from the corresponding hydroximic acid chlorides using a suspension of sodium bicarbonate. *Anti*:*syn* (**3**:**4**) product ratios were evaluated by ^{1}H NMR and by GC (for volatile products) or column chromatography and are given in Table 1.

Diazomethane (DZM) reacted slowly with **1** at room temperature (10 days) to afford good yields (90%) of an *anti*:*syn* adduct (**3a** and **4a**, respectively) mixture in a 75.5 (±0.5):24.5 (±0.5) ratio (measured by GC). Our finding confirms the results previously reported, several years ago, in a communication by Bergman and Keppel[15] and demonstrates that facial selectivity of the addition of **2a** to **1** is similar to that obtained for the reaction of **2a** with *cis*-3,4-dimethyl-1-methoxycarbonylcyclobutene (*anti*:*syn* = 72:28).[12] Thus, introduction of an electron withdrawing group on the C=C of **1** does not significantly affect the facial selectivity of its reaction with diazomethane.

Structures **3a** and **4a** were fully characterized by ^{1}H NMR (Table 2) and ^{13}C NMR data. In particular, the chemical shift difference between the two protons at position 4 is higher in the *syn* **4a** than in the *anti* adduct **3a** while H^5, H^6 and H^7 in **4a** resonate downfield with respect to the corresponding protons in **3a**. Moreover, $J_{5,6}$ and $J_{1,7}$ are consistently higher in the *syn* than in the *anti* adduct. These data closely parallel those reported previously for the *anti* and *syn* adducts obtained from the addition of **2a** to *cis*-3,4-dimethyl-1-methoxycarbonylcyclobutene.[12] *Syn* and *anti* stereochemistry of the adducts **4a** and **3a**, respectively, was confirmed by NOE experiments. Irradiation of the methyl group attached to C^6 in **3a** and **4a** increased the intensity of the H$^4_{endo}$ signal by 5% and left the H^5 signal unchanged in **4a**, while the opposite was observed in **3a** (the H$^4_{endo}$ signal was left unperturbed and the H^5 signal was increased by 6%).

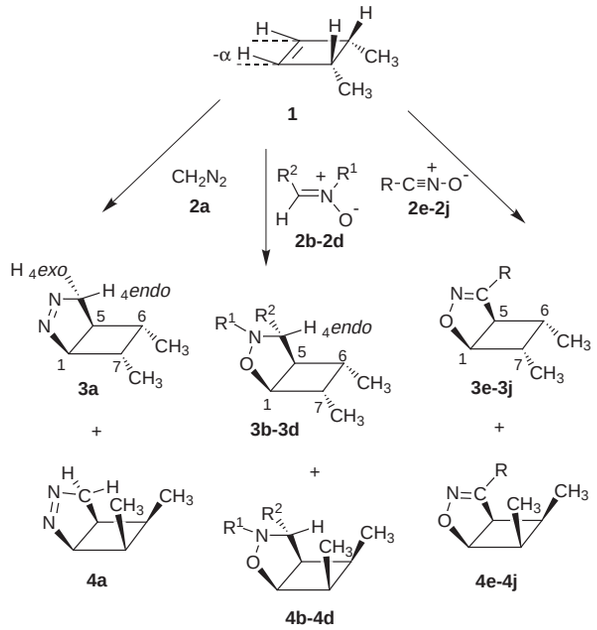

Scheme 1

Table 1 Facial selectivity in 1,3-dipolar cycloadditions to **1**

1,3-Dipole	**2**	Yield (%)	**3** (*Anti*) (%)	**4** (*Syn*) (%)
$CH_2=\overset{+}{N}=\bar{N}$	**a**	90	75	25
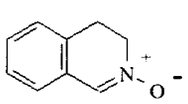	**b**	30 95	≥99 ≥99	— —
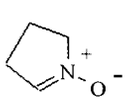	**c**	75	≥99	—
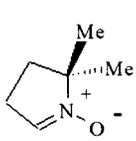	**d**	81	≥99	—
PhCNO	**e**	98	65	35
p-O_2N-C_6H_4-CNO	**f**	91	60	40
PhCOCNO	**g**	98	50	50
CH_3COCNO	**h**	95	50	50
Me_3CCNO	**i**	99	87	13
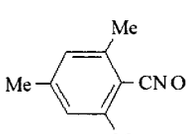	**j**	95	92	8

NOE experiments definitely confirm that the isolated adducts derive from an *anti-exo* transition state. Irradiation of H^4 in **3b** increased the H^6 signal intensity by 6%, while saturation of H^4 in **3d** gave rise to a higher NOE effect for the signal of H^6 (4%) than for the methyl group at C^6 (1%).

The reactions of 3,4-dihydroisoquinoline *N*-oxide (**2b**), 1-pyrroline *N*-oxide (**2c**) and 5,5-dimethyl-1-pyrroline *N*-oxide (**2d**) with **1** were 100% diastereoselective, within the limits of the analytical techniques used, to afford only the *anti-exo* adduct (**3b**, **3c** and **3d**, respectively). No evidence of the presence of the *syn-endo* or *syn-exo* adducts or of the *anti-endo* adduct was detected by ^{1}H NMR analysis of the crude reaction mixtures.

The reaction of **2b** with *cis*-3,4-dimethyl-1-methoxycarbonylcyclobutene has been reported[12] to be slightly less diastereoselective, as small amounts of the *syn* adduct (6%) could be isolated.

Assignment of *anti* stereochemistry to the adducts **3b**–**3d** is based on the small value of the vicinal coupling constants ($J_{1,7}$ = 2.9 and $J_{5,6}$ = 4.1 Hz in **3b**, $J_{1,7}$ = 2.7 and $J_{5,6}$ = 4.4 Hz in **3c** and $J_{1,7}$ = 2.7 and $J_{5,6}$ = 4.6 Hz in **3d**) involving the cyclobutane protons while the *trans* relationship between H^4 and H^5 is likewise suggested by the low value of the related *J* ($J_{4,5}$ = 2.4 Hz in **3b**, $J_{4,5}$ = 2.9 Hz in **3c** and $J_{4,5}$ < 0.5 Hz in **3d**).

Addition of nitrile oxides (**2e**–**2j**) to cyclobutene **1** showed a wide range of facial selectivity, going from a high *anti* selectivity for the addition of **2j**, to a slight prevalence of *anti* attack in the case of benzo (*anti*:*syn* = 65:35) (**2e**) and *p*-nitrobenzonitrile

Table 2 ^{1}H NMR data [δ ($CDCl_3$) in ppm and *J* in Hz] for *anti* (**3**) and *syn* (**4**) adducts of diazomethane (**2a**), 3,4-dihydroisoquinoline *N*-oxide (**2b**), pyrroline *N*-oxide (**2c**), 5,5-dimethylpyrroline *N*-oxide (**2d**) with **1**

Comp.	H^1	H$^4_{endo}$	H$^4_{exo}$	H^5	H^6	H^7	Me^6	Me^7	$J_{1,4exo}$	$J_{1,4endo}$	$J_{1,5}$	$J_{1,6}$	$J_{1,7}$	$J_{4exo,4endo}$	$J_{4exo,5}$	$J_{4endo,5}$	$J_{5,6}$	$J_{5,7}$	$J_{6,7}$	J_{6,Me^6}	J_{7,Me^7}
3a	4.77	4.50	4.45	2.15	1.81	2.42	1.00	1.22	2.0	3.2	6.4	1.0	4.6	18.0	7.6	3.0	5.5	1.2	9.0	7.1	7.3
4a	5.20	4.69	4.28	2.68	2.63	3.15	0.67	0.87	2.0	3.4	6.6	1.5	9.9	18.2	9.0	2.2	8.0	1.6	9.0	7.3	7.6
3b	4.17	4.39	—	2.89	2.49	2.55	1.10	0.99	—	<0.5	6.8	<0.5	2.9	—	—	2.4	4.1	1.2	7.3	7.1	7.3
3c	4.15	3.47	—	2.71	2.56	2.27	0.97	0.94	—	<0.5	6.6	<0.5	2.7	—	—	2.9	4.4	1.2	9.8	7.3	7.6
3d	4.07	3.53	—	2.57	2.19	2.20	0.88	0.86	—	<0.5	6.6	<0.5	2.7	—	—	<0.5	4.6	1.2	9.9	7.3	7.6

Table 3 ^{1}H NMR data [δ ($CDCl_3$) in ppm and J in Hz] for *anti* (**3**) and *syn* (**4**) adducts of nitrile oxides (**2e**–**2j**) with **1**

Comp.	H^1	H^5	H^6	H^7	Me^6	Me^7	$J_{1,5}$	$J_{1,6}$	$J_{1,7}$	$J_{5,6}$	$J_{5,7}$	$J_{6,7}$	J_{6,Me^6}	J_{7,Me^7}
3e	4.82	3.76	2.68	2.82	1.06	1.24	7.8	<0.5	4.4	3.2	1.5	9.3	7.3	7.6
4e	5.17	4.30	[a]	[a]	0.81	1.02	7.6	1.4	6.1	7.8	2.7	[a]	7.1	7.3
3f	4.91	3.77	2.68	2.86	1.09	1.27	7.8	<0.5	4.4	3.2	1.4	9.3	7.3	7.6
4f	5.28	4.31	3.30	3.30	0.79	1.03	7.6	1.2	6.1	7.6	2.7	9.0	7.1	7.3
3g	4.84	3.79	2.70	2.84	1.08	1.21	7.6	<0.5	4.1	3.2	1.7	9.3	7.3	7.3
4g	5.24	4.34	2.95	3.00	0.88	1.05	7.6	1.2	6.1	7.6	3.4	9.0	7.1	7.3
3h	4.84	3.52	2.56	2.76	1.04	1.15	7.6	<0.5	4.1	3.2	1.7	9.3	7.3	7.3
4h	5.30	4.06	2.93	2.93	0.82	0.96	7.6	2.2	5.9	7.6	3.4	9.0	7.1	7.3
3i	4.57	3.40	2.70	2.65	1.02	1.11	7.6	<0.5	3.1	3.6	1.2	~9.0	7.0	7.3
4i	4.80	3.82	2.85	2.85	0.96	1.00	[b]	[b]	[b]	[b]	[b]	[b]	7.3	7.3
3j	4.84	3.64	2.57	2.93	1.05	1.07	7.6	<0.5	4.9	2.7	1.5	9.0	7.3	7.3
4j	5.15	4.40	2.50	2.87	0.80	1.14	7.6	1.9	5.6	7.6	2.7	9.2	7.0	7.3

[a] Buried under the signals of the main diastereoisomer. [b] Second order ABX spectra.

Table 4 Calculated activation parameters[a] and TS dipole moments (B3LYP/6-31G*), calculated and experimental *anti*:*syn* ratios for the 1,3-dipolar cycloaddition of HCNO, CH_2N_2 and CH_2=N(O)H, respectively, with **1**

1,3-Dipole	TS	$\Delta E^{\ddagger}$	$\Delta\Delta E^{\ddagger}$[b]	$\Delta H^{\ddagger}$	$\Delta S^{\ddagger}$[c]	$\Delta G^{\ddagger}$	$\Delta\Delta G^{\ddagger}$	Calc. *anti*:*syn*	Exp. *anti*:*syn*	Dipole moment/ Debye
HCNO	*Syn*	53.72	0.29	57.45	−126.94	95.27	0.38	54:46	63:35[d]	2.49
	Anti	54.01		57.86	−124.22	94.89			50:50[e]	2.47
CH_2N_2	*Syn*	74.10	3.14	80.00	−127.53	117.99	3.77	82:18	76:24	1.96
	Anti	70.96		76.82	−125.48	114.22				1.98
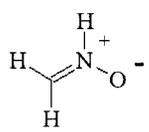	*Syn-endo*	87.15		—	—	—				2.74
	Syn-exo	57.32	8.62[f]	63.09	−143.72	105.94	8.75	97:3	≥99[g]	2.67
	Anti-endo	81.59		—	—	—				2.78
	Anti-exo	48.70		54.35	−143.18	97.19				2.60

[a] Energies in kJ mol^{-1}, entropy in J K^{-1} mol^{-1}; standard state (298 K) of the molar concentration scale. [b] $\Delta\Delta E^{\ddagger} = \Delta E^{\ddagger}(syn) - \Delta E^{\ddagger}(anti)$; $\Delta\Delta G^{\ddagger} = \Delta G^{\ddagger}(syn) - \Delta G^{\ddagger}(anti)$. [c] Reaction statistical factors are included. [d] Experimental ratio for benzonitrile oxide cycloaddition. [e] Experimental ratio for pyruvonitrile oxide (**2h**) and phenylglyoxylonitrile oxide (**2g**) cycloadditions. [f] $\Delta\Delta E^{\ddagger} = \Delta E^{\ddagger}(syn\text{-}exo) - \Delta E^{\ddagger}(anti\text{-}exo)$. [g] Experimental ratio for cycloadditions of nitrones **2b**–**2d**.

oxide (**2f**) to a complete absence of facial selectivity for the addition of phenylglyoxylonitrile oxide and pyruvonitrile oxide (**2g** and **2h**, respectively) (Table 1).

For the sake of comparison in the reaction of benzonitrile oxide and phenylglyoxylonitrile oxide with *cis*-3,4-dimethyl-1-methoxycarbonylcyclobutene *syn* attack is slightly dominant (*anti*:*syn* = 45:55 and 39:61, respectively).[12]

Anti or *syn* stereochemistry of adducts **3e**,**4e**–**3j**,**4j** has been assigned on the basis of the following ^{1}H NMR spectroscopic evidence: (1) chemical shifts of H^1 and H^5 in *anti* adducts are always lower by ≥0.25 ppm than those of the corresponding protons in *syn* adducts; (2) both the vicinal ($J_{5,6} \approx 7.6$–7.8 Hz and $J_{1,7} \approx 5.6$–6.1 Hz) and long range ($J_{1,6} \approx 1.2$–2.2 Hz and $J_{5,7} \approx 2.7$–3.4 Hz) cross coupling constants in *syn* adducts (**4e**–**4j**) are significantly and consistently higher than the corresponding constants ($J_{5,6} \approx 2.7$–3.6 Hz, $J_{1,7} \approx 3.1$–4.9 Hz, $J_{1,6}$ <0.5 Hz and $J_{5,7} \approx 1.2$–1.7 Hz) in *anti* adducts (**3e**–**3j**) (see Table 3); (3) in the case of *syn* adducts (**4e**–**4j**) the methyl groups at position 6 (both hydrogens and carbons) resonate upfield with respect to the corresponding methyl group in *anti* adducts (**3e**–**3j**) (Table 3) owing to the deshielding effect of the =C–R part of the isoxazoline moiety.

Discussion

The clear-cut dominance of the *anti* attack in the reactions of diazomethane **2a**, nitrones **2b**–**2d** and nitrile oxides **2i**, **2j** is no doubt the result of steric repulsion between the attacking 1,3-dipole and the methyl groups of the dipolarophile. The highest steric effects are observed in the reaction of nitrones, while steric encumbrance of the "small" diazomethane felt by the methyl groups of **1** approaches that of the bulkiest nitrile oxides.

However, when steric encumbrance of the 1,3-dipole decreases as in nitrile oxides **2e** and **2f** and even more in the case of **2g** and **2h** (in which the C=O group acts as a spacer bringing the methyl and phenyl group, respectively, away from the crowded zone of the transition state) the presence of a small *syn* directing effect emerges. In the case of the reaction of **2g** and **2h** this effect perfectly balances repulsive steric interactions.

The small *syn* pyramidalization of the olefinic carbons of **1** (mentioned in the Introduction and confirmed by higher level calculations: $\alpha = -1.0°$ and $-1.1°$ at the HF/6-31G* and at the B3LYP/6-31G* level, respectively) with the related bending energy asymmetry ($E_{+20°} - E_{-20°} = 2.76$ and 2.38 kJ mol^{-1}, respectively) lends itself as a reasonable explanation for this factor. A similar effect can be held responsible for the slight prevalence of *syn* attack by nitrile oxides **2e** and **2h** to *cis*-3,4-dimethyl-1-methoxycarbonylcyclobutene.[12]

The very low dipole moment of **1** (≤0.14 D)† tells us that electrostatic interactions are not important in controlling the facial selectivity of its reactions. This argument is substantiated by the finding that the calculated dipole moments (Table 4) of the *syn* and *anti* transition structures are very similar to each other for all three 1,3-dipoles studied.

Thus, the observation that facial selectivity of **1** is similar to that of *cis*-3,4-dimethyl-1-methoxycarbonylcyclobutene (however with a slight increase of *syn* selectivity in the reactions of nitrile oxides **2b**, **2e** and **2g**) seems to substantiate our previous suggestion that introduction of a methoxycarbonyl group on a double bond does not heavily change face selectivity when electrostatic interactions are absent.[16]

† 0.08 D and 0.14 D at HF/6-31G* and B3LYP/6-31G* level, respectively.

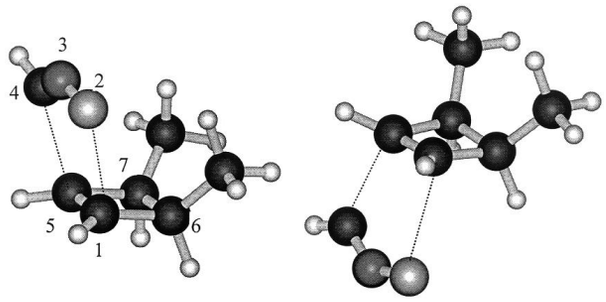

Fig. 1 *Syn* and *anti* TSs (B3LYP/6-31G*) for the cycloaddition reaction of formonitrile oxide (HCNO) with cyclobutene **1**.

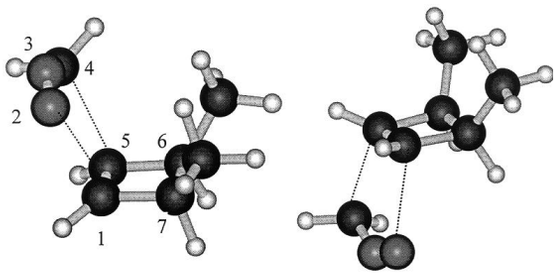

Fig. 2 *Syn* and *anti* TSs (B3LYP/6-31G*) for the cycloaddition reaction of diazomethane (CH_2N_2) with cyclobutene **1**.

Computational study

Results and discussion

The different selectivity observed for the 1,3-dipoles studied is almost certainly only the result of differential steric effects. Thus, it was of interest to calculate transition structures to find out how steric interactions are reflected in their geometry and in their energy, trying to understand why the steric effect reaches its maximum in the reaction of nitrones. The latter observation holds not only for the 1,3-dipolar cycloadditions to **1** and its methoxycarbonyl derivative but also for those to the other *cis*-3,4-disubstituted cyclobutenes studied by us.

The fact that these systems are amenable to good level calculations at a reasonable cost led us to perform, for the simplest cycloaddition reactions of **1** with HCNO (formonitrile oxide), CH_2N_2 (DZM) and CH_2=N(O)H (nitrone), *ab initio* calculations with both the HF/6-31G* and B3LYP/6-31G* methods in order to produce not only geometries but also reliable energies.

We were able to locate the *syn* and *anti* transition structures (TSs) for the reaction of formonitrile oxide (see Fig. 1) and DZM (Fig. 2) as well as the four TSs (*syn-endo*, *anti-endo*, *syn-exo* and *anti-exo*) for the reaction of nitrone (Fig. 3).

The electronic activation energies ($\Delta E^{\ddagger}$) as well as the thermodynamic activation parameters (*i.e.*, activation enthalpies, activation entropies and activation free enthalpies in the gas phase and referenced to the standard state (298 K) of the molar concentration scale),[17] obtained with the B3LYP/6-31G* method, are gathered in Table 4.

The absolute values of B3LYP activation free enthalpies ($\Delta G^{\ddagger} \leq 118$ kJ mol^{-1}) are in good agreement with the experimental data for 1,3-dipolar cycloadditions (<125 kJ mol^{-1}) while the calculated activation entropies (124–143 J K^{-1} mol^{-1}) are also reasonably consistent with the observed values (≈125 J K^{-1} mol^{-1}).[18]

It is gratifying that the relative activation free enthalpies ($\Delta\Delta G^{\ddagger}$) correctly reproduce the experimental trend in facial selectivity, *i.e.*, mixture of isomers with *anti* attack dominating, which increases on going from formonitrile oxide to nitrone. Moreover, contributions of nuclear motions to the activation free enthalpy for *anti* TSs are similar to those for the corresponding *syn* TSs so that the differences between

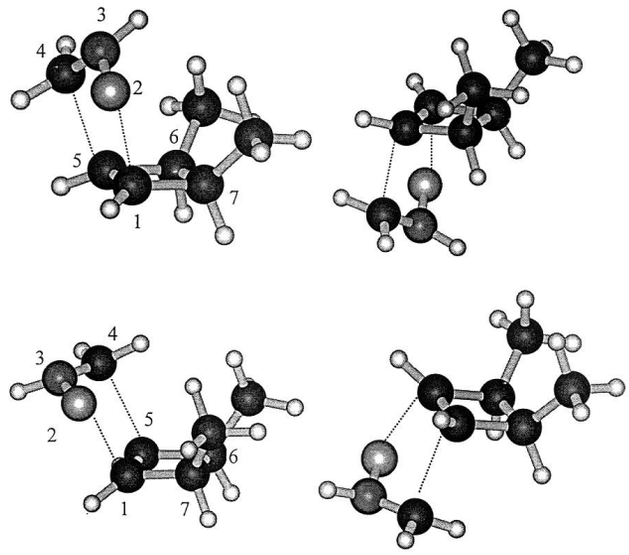

Fig. 3 From top left to right: *syn-endo*, *anti-endo*, *syn-exo* and *anti-exo* TSs (B3LYP/6-31G*) for the cycloaddition reaction of methyleneamine *N*-oxide [H_2C=N(O)H] with cyclobutene **1**.

the electronic activation energies ($\Delta\Delta E^{\ddagger}$) are also in reasonable accord with the experimental diastereoselectivity (Table 4).

As for the four TSs of nitrone cycloaddition, the two *endo* TSs exhibit a much higher energy (by at least 30 kJ mol^{-1}, as a result of more severe steric repulsions) than the two *exo* TSs (Table 4) and, consequently, their contribution to product distribution can be neglected. This is obviously true not only for the parent nitrone but even more for nitrones **2b**–**2d**. We also feel that the difference in steric interactions between the *anti-exo* and the *syn-exo* pathways does not change substantially on going from the parent nitrone to nitrones **2b**–**2d**, because the substituents in cyclic nitrones are positioned far from the methyl groups of the cyclobutene.

Therefore, comparison between calculated and experimental data for nitrone reactions is certainly meaningful and this is also true for nitrile oxide cycloadditions.

In fact, the relative activation free enthalpy ($\Delta\Delta G^{\ddagger}$) of the formonitrile oxide cycloaddition reproduces the experimental trend in facial selectivity of phenylglyoxylonitrile oxide, pyruvonitrile oxide and benzonitrile oxide (**2g**, **2h** and **2e** respectively), suggesting that the steric influence of the substituent on the nitrile oxide is small, particularly when the substituent can be coplanar to the 1,3-dipolar moiety in the TS. This is not the case of nitrile oxides **2i** and **2j** which show high (but not complete) *anti* facial selectivity.

To the best of our knowledge this is the first study of diastereofacial selectivity in 1,3-dipolar cycloaddition with DFT theory (see ref. 19–21 for previous DFT calculations on 1,3-dipolar cycloadditions).

With respect to correlated calculations, the HF/6-31G* method slightly increases the difference between the activation electronic energies ($\Delta\Delta E^{\ddagger} = 1.51$, 4.81 and 10.88 kJ mol^{-1} for HCNO, DZM and nitrone cycloadditions, respectively) as well as between the activation free enthalpies ($\Delta\Delta G^{\ddagger} = 2.30$, 5.94 and 11.05 kJ mol^{-1} for HCNO, DZM and nitrone cycloadditions, respectively) of the competing *syn* and *anti* pathways. However, a substantial agreement between calculated and experimental selectivity is maintained.

As for absolute values, the activation entropies ($\Delta S^{\ddagger}$) calculated from HF frequencies (−121.13 and −118.62 J K^{-1} mol^{-1}, respectively, for *syn* and *anti* TSs of HCNO cycloaddition; −138.49 and −135.65 J K^{-1} mol^{-1}, respectively, for *syn* and *anti* TSs of DZM cycloaddition) are similar to those calculated with the B3LYP metod, while the electronic activation energies increase by ≈84 kJ mol^{-1} (*e.g.*, $\Delta E^{\ddagger} = 143.64$ and 142.13 kJ

Table 5 Geometry parameters (B3LYP/6-31G*) for the transition structures of the reactions of HCNO, CH_2N_2 and nitrone with **1**

Dipole	TS	α_1[a]	α_2[a]	β_1[b]	β_2[b]	C^1–C^5	C^1–X^2	C^4–C^5	H^4_{endo}–Me^6	H^4_{endo}–H^6
HCNO	*Syn*	−14.0	−28.5	108.5	111.5	1.376	2.494	2.237	—	—
	Anti	11.1	25.7	−103.0	−106.2	1.374	2.469	2.223	—	—
CH_2N_2	*Syn*	−23.4	−33.8	109.7	113.8	1.385	2.386	2.266	2.366	—
	Anti	19.7	30.4	−103.6	−107.6	1.383	2.367	2.257	—	2.530
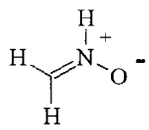	*Syn-endo*	−17.6	−33.1	109.8	115.4	1.377	2.419	2.170	2.678	—
	Syn-exo	−24.3	−35.4	111.7	114.4	1.390	2.219	2.229	2.091	—
	Anti-endo	12.6	28.8	−101.4	−107.7	1.374	2.403	2.168	—	2.740
	Anti-exo	20.5	30.7	−104.8	−106.1	1.388	2.200	2.223	—	2.156

[a] Defined as follows: $\alpha_1 = \pm(180° - |H^1C^1C^5C^7|)$ and $\alpha_2 = \pm(180° - |H^5C^5C^1C^6|)$, using a plus sign when olefinic hydrogens are bent towards the methyl groups, and a negative when they are bent in the opposite (*anti*) direction (see Scheme 2). [b] Defined as follows: $\beta_1 = \pm|XC^1C^5C^7|$ and $\beta_2 = \pm|C^4C^5C^1C^6|$, using a plus sign when the 1,3-dipole is *syn* with respect to the methyl groups, and a negative sign when it is *anti* (see Scheme 2).

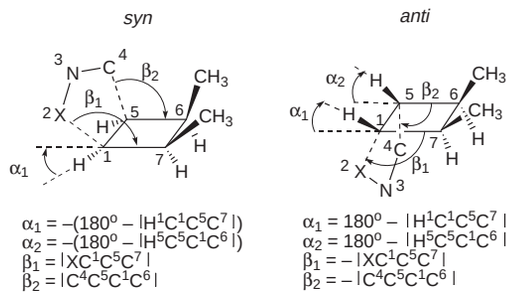

Scheme 2

mol^{-1}, respectively, for *syn* and *anti* HCNO TSs; 151.96 and 147.15 kJ mol^{-1}, respectively, for *syn* and *anti* DZM TSs). As a result, the HF activation free enthalpies look too high in comparison with the DFT values and they cannot reproduce the experimental reaction rate of the 1,3-dipoles.

It should be emphasized that calculated gas phase selectivity for the 1,3-dipolar cycloadditions under study can be meaningfully compared to experimental condensed phase selectivity as the dipole moments of *syn* and related *anti* TSs are almost exactly the same (Table 4) thus suggesting that solvation effects should not influence product distribution.

Syn and *anti* transition structures (Figs. 1, 2 and 3) correspond to early TSs in terms of bond breaking and bond making.

Looking at the geometry of the TSs, a comparison between HF/6-31G* and DFT calculations reveals that DFT TSs (Table 5, Figs. 1, 2 and 3) always exhibit longer incipient bond lengths than the corresponding HF TSs‡ and that this difference is more pronounced for the C^1–X^2 bonds than for the C^4–C^5 bonds. As a result, forming bond length asynchrony predicted by HF calculations for TSs of DZM and HCNO cycloadditions (with C^4–C^5 shorter than C^1–X^2) is enhanced on passing to DFT calculations while asynchrony is reduced in the case of the *syn-exo* and *anti-exo* TSs (for which the HF method foresees the C^1–X^2 bond shorter than C^4–C^5 bond) of nitrone cycloaddition.§

Other geometrical parameters obtained by the two methods are very similar and, even more importantly, geometry differences between *syn* TSs and their *anti* counterparts are independent of the method of calculation. Thus we can confidently discuss facial selectivity on the basis of these differences attributing them to real effects and not to artifacts from calculations.

The tendency to relieve as far as possible steric interactions between the attacking 1,3-dipole and the methyl groups of the dipolarophile does clearly emerge in the slants (see the improper torsion angles $\beta_1 = XC^1C^5C^7$ and $\beta_2 = C^4C^5C^1C^6$ which are listed in Table 5 and Scheme 2) of the forming bonds which are larger by ≈6° in the *syn* attack than in the *anti* attack, as well as in the "outside inclination" of the two C^6–Me and C^7–Me bonds which also is higher by 4–6° in the *syn* TSs than in the related *anti* TSs.

The larger inclination of the 1,3-dipole *syn* approach with respect to the *anti* one is accompanied by a higher out-of-plane deformation of the olefinic hydrogens (see α_1 and α_2 in Table 5 and Scheme 2). This deformation is larger by ≈3–4° in the *syn* than in the corresponding *anti* TSs,¶ however it can take place practically without a higher energy cost. In fact, the *anti* bending of the olefinic hydrogens (induced by *syn* attack) is intrinsically easier than *syn* bending (induced by *anti* attack).

As emphasized above, this *syn* orienting effect exactly and accidentally compensates for *anti* orienting factors (steric in origin) in the cycloadditions of the less encumbered nitrile oxides (*i.e.*, **2g** and **2h**).

In the case of DZM and nitrone reactions H^4_{endo} points inside and in the *syn* TS it is close enough to the methyl group at position 6 (in particular in the case of nitrone, *i.e.*, $H^4 \cdots H\text{-}CH_2\text{-} \approx 2.09$ Å in the nitrone *syn-exo* TS and ≈2.37 Å in the DZM *syn* TS), to give rise to additional destabilizing crowding.

However, the complete *anti* selectivity of the nitrone attack on **1** deserves further comment. It is well known that the approach geometry of allenyl- or propargyl-type 1,3-dipoles (propargyl is prop-2-ynyl) (*e.g.*, DZM and HCNO) to dipolarophiles is intrinsically different from that of allyl-type 1,3-dipoles (*e.g.*, nitrone).[18] In our study, on passing from the ground state to the TS the heavy atoms of DZM and HCNO change from a linear to a bent array while practically remaining in the same plane of the incipient bonds (dihedral angle between the CNX plane and the incipient bond plane >175°).

The attack by nitrone features an almost "parallel planes" (the CNO nitrone plane and the double bond dipolarophile

‡ HF/6-31G* calculations predict the following C^1–X^2 bond lengths: 2.320, 2.304 Å in the *syn* and *anti* TSs for HCNO cycloaddition, 2.293, 2.274 Å in the *syn* and *anti* TSs for DZM cycloaddition and 2.089, 2.084 Å in the *syn-exo* and *anti-exo* TSs for nitrone cycloaddition, respectively. HF/6-31G* calculations predict the following C^4–C^5 bond lengths: 2.156, 2.141 Å in the *syn* and *anti* TSs for HCNO cycloaddition, 2.190, 2.179 Å in the *syn* and *anti* TSs for DZM cycloaddition and 2.223, 2.201 Å in the *syn-exo* and *anti-exo* TSs for nitrone cycloaddition, respectively.

§ DFT calculations predict slightly shorter bond length also for products (*e.g.*, by ≈0.020 Å and 0.005 Å for the C^1–N and C^4–C^5 bonds, respectively, in pyrazolines **3a** and **4a**). However, all in all, one can say that DFT calculations predict slightly earlier TSs than HF calculations.

¶ It should be stressed that the geometry details of the 1,3-dipole moiety are the same in both *syn* and related *anti* TSs (the bending angles of H-**CNO** and H_2**CNN** are 143° and 145°, respectively, in both TSs). At variance with what was observed by us in the *syn* and *anti* transition structures for 1,3-dipolar cycloadditions on norbornene, *cis*-3,4-dichlorocyclobutene, bicyclopentene *etc.* the 1,3-dipole deformation does not play any role in determining the facial selectivity of the 1,3-dipolar cycloadditions on **1**.[8–10]

plane) orientation complex followed, on going to the TS, by pyramidalization of the nitrogen atom which also moves upward. The resulting angle between the CNO plane and the plane of the incipient bonds in the TS is not far from 130°. This underlines that when comparing *syn* and *anti* attack by the nitrone on **1** it is also important to take into account the orientation of the CNO nitrone plane with respect to the dipolarophile. For example, the dihedral angle between the CNO plane and the cyclobutene plane increases from 156° in the unencumbered *exo-anti* TS to 166° in the *syn-exo* TS. A widening of this angle in the *syn* TS, with respect to the "ideal" value of 156°, is necessary in order to make H^4 move upward and to avoid a too close contact between this hydrogen and the methyl group at position 6.

Once again, relief of steric interactions gives rise to a TS geometry deformation which is now present only in the nitrone reactions. This aspect contributes to increase the *syn-exo* TS energy and to enhance the *anti* selectivity of this reaction with respect to the DZM and HCNO reactions.

To conclude, both HF/6-31G* and B3LYP/6-31G* calculations give a satisfactory answer to the facial selectivity problem while TS geometries show that significant steric interactions are operative in the *syn* attack and that they become progressively higher on passing from nitrile oxide, to diazomethane and to nitrone.

Experimental

Melting points are uncorrected. Elemental analyses were made on a Carlo Erba CNH analyzer, model 1106. Infrared spectra were recorded as KBr discs or films on a Perkin-Elmer FT1000 spectrophotometer. ^{1}H and ^{13}C NMR spectra were recorded on a Bruker AE 300 spectrometer with Me_4Si as internal standard. The chemical shift of aromatic protons as well as the CH_2s of the tetrahydroisoquinoline, pyrroline *N*-oxide, 5,5-dimethylpyrroline *N*-oxide moieties of the adduct from the reaction of **2b**, **2c** and **2d** are not reported. Protons were correlated by decoupling and COSY experiments, while protons were correlated to carbons by ^{1}H–^{13}C heterocorrelated spectra. GC analyses were performed with a DANI 6500, PTV injector, CP-Sil 19CB (25m) capillary column using H_2 as a carrier. Preparative column chromatography was performed on Merk Silicagel 60 (79–230 mesh) using cyclohexane–ethylacetate mixtures (from 95:5 to 60:40) unless otherwise stated. *cis*-3,4-Dimethylcyclobutene **1**,[14] diazomethane **2a**, 3,4-dihydroisoquinoline *N*-oxide **2b**,[22] and the precursor of the nitrile oxides **2g**–**2i**, and the nitrile oxide **2j**[23,24] were prepared according to published procedures.

Reaction of diazomethane (2a)

The cycloaddition reaction of **1** (100 mg, 50% in diglyme) with **2a** was carried out in ethyl ether at room temperature using an excess (≥2 equiv.) of 1,3-dipole, and adding every 4 days a freshly made solution of **2a**. After 10 days the dipolarophile was almost completely consumed (GC analysis). The solvent was removed at 0 °C with a rotavapor, and the oily residue was purified by column chromatography (eluent *n*-pentane–diethyl ether = 85:15) to give **3a** and **4a** as colorless oils.

Syn:*anti* ratios were evaluated by ^{1}H NMR and GC analysis on the crude reaction mixture.

Adduct 3a. Colorless oil. ^{13}C NMR δ ($CDCl_3$) 14.25 (CH_3), 15.00 (CH_3), 34.56 (CH), 36.11 (CH), 36.77 (CH), 83.32 (CH_2), 92.57 (CHN). IR (KBr) 2961, 2924, 2871, 1533, 1463, 1430, 1381, 1276, 1186, 1093, 917 cm^{-1}.

Adduct 4a. Colorless oil. ^{13}C NMR δ ($CDCl_3$) 9.29 (CH_3), 10.56 (CH_3), 30.90 (CH), 31.21 (CH), 36.06 (CH), 77.61 (CH_2), 89.82 (CHN). IR (KBr) 2961, 2928, 2871, 1534, 1463, 1430, 1380, 1331, 1278, 1199, 1155, 1119, 1093, 918 cm^{-1}.

Reaction of 3,4-dihydroisoquinoline *N*-oxide (2b)

A solution of **2b** (123 mg, 0.84 mmol) and an excess of **1** (206 mg, 55%, 13.8 mmol) in 2.5 ml of benzene was left in a vial at 80 °C for 2 days. Evaporation of the solvent afforded in a good yield (95%) the adduct **3b**. This reaction was also carried out at room temperature for 6 days. Once again **3b** was the only detectable product in 30% yield.

Adduct 3b. Colorless oil. Anal. Calc. for $C_{15}H_{19}NO$: C, 78.6; H, 8.4; N, 6.1. Found: C, 78.8; H, 8.3; N, 6.2%. ^{13}C NMR δ ($CDCl_3$) 12.80 (CH_3), 15.42 (CH_3), 24.36 (CH_2), 31.78 (CH), 36.72 (CH), 48.46 (CH_2N), 57.79 (CH), 67.34 (CHN), 81.61 (CHO), 126.12 (CH arom.), 126.36 (CH arom.), 127.17 (CH arom.), 128.33 (CH arom.), 133.63 (Cq, arom.), 135.85 (Cq arom.). IR (KBr) 3018, 2954, 1578, 1453, 1052, 1038, 744 cm^{-1}.

Reaction of 1-pyrroline *N*-oxide (2c)

A solution of **2c** (80 mg, 0.94 mmol) and **1** (50 mg, 51%, 0.31 mmol, 49% of diglyme) in 0.5 ml of benzene was left in a vial at room temperature for 5 days. Evaporation of the solvent and purification by column chromatography on silica gel (eluent cyclohexane–ethyl acetate = 80:20) afforded 39 mg of the adduct **3d** (75% yield).

Adduct 3c. Colorless oil. Anal. Calc. for $C_{10}H_{17}NO$: C, 71.8; H, 10.2; N, 8.4. Found: C, 71.5; H, 10.0; N, 8.3%. ^{13}C NMR δ ($CDCl_3$) 12.79 (CH_3), 15.23 (CH_3), 24.55 (CH_2), 30.01 (CH_2), 31.75 (CH), 36.57 (CH), 56.37 (CH_2), 56.46 (CH), 71.72 (CH), 81.99 (CH). IR (KBr) 2954, 2926, 2869, 1462, 1447, 1379, 1260, 1100, 1038, 805 cm^{-1}.

Reaction of 5,5-dimethylpyrroline *N*-oxide (2d)

A solution of **2d** (67 mg, 0.6 mmol) and **1** (50 mg, 50% of diglyme, 0.31 mmol) in 2 ml of benzene was left in a vial at 80 °C for 8 days. Evaporation of the solvent and purification by column chromatography on silica gel (eluent cyclohexane–acetate = 75:25) afforded 49 mg of the adduct **3d** (81% yield).

Adduct 3d. Colorless oil. Anal. Calc. for $C_{12}H_{21}NO$: C, 73.8; H, 10.8; N, 7.2. Found: C, 73.6; H, 10.7; N, 7.2%. ^{13}C NMR δ ($CDCl_3$) 12.81 (CH_3), 14.96 (CH_3), 24.31 (CH_3), 27.78 (CH_3), 30.31 (CH_2), 31.67 (CH), 35.72 (CH_2), 36.46 (CH), 56.71 (CH), 68.28 (CH), 69.41 (CH), 81.25 (CH). IR (KBr) 3018, 2954, 1578, 1453, 1052, 1038, 744 cm^{-1}.

Reaction of nitrile oxides (2e–2j)

Nitrile oxides **2e**–**2j** were generated *in situ* from the related hydroximic acid chloride. A solution of the hydroximic acid chloride (0.8 mmol) and a slight excess of **1** (1 mmol) in benzene (5 ml) was stirred at room temperature from 6 to 12 h as a function of the hydroximic acid chloride used (see Table 1), in presence of an 100% excess of solid $NaHCO_3$ (1.6 mmol). The inorganic salts were filtered off, the solvent evaporated and the mixture of diastereoisomers was purified by column chromatography. The diastereoisomer ratios were evaluated by ^{1}H NMR and in the case of **3e**, **4e**, **3h**, **4h** and **3i**, **4i** diastereoisomers could not be obtained in a pure state by column chromatography.

Adduct 3f. Pale yellow crystalline solid from cyclohexane–ethyl acetate = 85:15. Mp 168.0–168.5 °C. Anal. Calc. for $C_{13}H_{14}N_2O_3$: C, 63.4; H, 5.7; N, 11.4. Found: C, 63.1; H, 5.6; N, 11.2%. ^{13}C NMR δ ($CDCl_3$) 12.53, 16.06, 35.26, 39.89, 53.52, 86.22, 124.09, 127.45, 135.20, 148.44, 158.61. IR (KBr) 1607, 1598, 1561, 1514, 1343, 893, 853 cm^{-1}.

Adduct 4f. Pale yellow crystalline solid from methanol. Mp 161.0–162.8 °C. Anal. Calc. for $C_{13}H_{14}N_2O_3$: C, 63.4; H, 5.7; N, 11.4. Found: C, 63.2; H, 5.7; N, 11.3%. ^{13}C NMR δ ($CDCl_3$) 8.85, 11.58, 33.70, 38.91, 51.20, 82.27, 123.88, 127.52, 136.62, 148.33, 157.38. IR (KBr) 1599, 1559, 1514, 1345, 894, 853 cm^{-1}.

Adduct 3g. Colorless oil. Anal. Calc. for $C_{14}H_{15}NO_2$: C, 73.3; H, 6.6; N, 6.1. Found: C, 73.4; H, 6.6; N, 6.2%. ^{13}C NMR δ ($CDCl_3$) 12.55, 15.83, 36.23, 40.55, 53.82, 86.82, 128.34, 130.31, 133.45, 136.15, 161.29, 186.29. IR (KBr) 2962, 1654, 1553, 1448, 1362, 1253 cm^{-1}.

Adduct 4g. Colorless oil. Anal. Calc. for $C_{14}H_{15}NO_2$: C, 73.3; H, 6.6; N, 6.1. Found: C, 73.1; H, 6.5; N, 6.0%. ^{13}C NMR δ ($CDCl_3$) 9.05, 11.01, 34.08, 39.01, 52.28, 82.48, 128.33, 130.28, 133.36, 136.21, 160.26, 189.95. IR (KBr) 2964, 1654, 1556, 1449, 1363, 1217 cm^{-1}.

Adduct 3j. Colorless solid from cyclohexane mp 72.0–73.5 °C. Anal. Calc. for $C_{16}H_{21}NO$: C, 79.0; H, 8.7; N, 5.8. Found: C, 78.8; H, 8.6; N, 5.8%. ^{13}C NMR δ ($CDCl_3$) 12.54, 16.36, 20.00, 20.99, 33.17, 40.12, 58.64, 84.57, 125.99, 128.59, 130.31, 138.40, 160.45. IR (KBr) 2926, 1612, 1461, 1382, 978, 844, 825 cm^{-1}.

Adduct 4j. Colorless oil. Anal. Calc. for $C_{16}H_{21}NO$: C, 79.0; H, 8.7; N, 5.8. Found: C, 78.7; H, 8.5; N, 5.6%. ^{13}C NMR δ ($CDCl_3$) 9.23, 11.15, 20.92, 21.46, 29.69, 34.28, 38.49, 55.13, 79.83, 129.50, 130.08, 136.50, 138.03, 157.30. IR (KBr) 2930, 1611, 1463, 1382, 970 cm^{-1}.

Computational methods

Geometries for all the structures were obtained with both the HF/6-31G* and the B3LYP/6-31G* (Becke's three-parameter hybrid exchange functional in combination with the gradient corrected functional of Lee, Yang and Parr) methods as implemented in the Gaussian 94 suite of programs.[25] The search for TSs was limited to concerted transition structures and gradient geometry optimization and default threshold for convergence were used. Critical points of all the TSs, but *syn-endo* and *anti-endo* TSs, were fully characterized as first order saddle points by diagonalizing the Hessian matrices of the optimized structures. TSs were found to have only one negative eigenvalue, the corresponding eigenvector involving the expected formation of the two new bonds. Vibrational frequencies, in the harmonic approximation, were calculated for all the optimized structures (with the exception of *syn-endo* and *anti-endo* TSs) and used unscaled[17] to compute the zero point energies, their thermal corrections, the vibrational entropies and their contribution to activation enthalpies, entropies and free enthalpies. Activation parameters reported in Tables 4 and 5 are for gas phase reaction and referred to the standard state of molar concentrations (ideal mixture at 1 mol L^{-1} and 1 atm).[17]

Cartesian coordinates of all TSs are available on request.

Acknowledgements

Financial support from MURST and CNR is gratefully acknowledged.

References

1 M. Burdisso, A. Gamba, R. Gandolfi, L. Toma, A. Rastelli and E. Schiatti, *J. Org. Chem.*, 1990, **55**, 3311 and references cited therein.
2 K. Hassenrüch, H. Höchstetter, H. D. Martin, A. Steigel and H. P. Wingen, *Chem. Ber.*, 1987, **120**, 203.
3 H. Landen, B. Margraf and H. D. Martin, *Tetrahedron Lett.*, 1988, **29**, 6593.
4 H. Landen, B. Margraf, H. D. Martin and A. Steigel, *Tetrahedron Lett.*, 1988, **29**, 6597.
5 H. Hake, H. Landen, B. Margraf, H. D. Martin, B. Mayer, A. Steigel, G. Distefano and A. Modelli, *Tetrahedron Lett.*, 1988, **29**, 6601.
6 J. I. G. Cadogan, D. K. Cameron, I. Gosney, E. J. Tinley, S. J. Wyse and A. Amaro, *J. Chem. Soc.*, *Perkin Trans. 1*, 1991, 2081.
7 A. Rastelli, M. Burdisso and R. Gandolfi, *J. Phys. Org. Chem.*, 1990, **3**, 159.
8 A. Rastelli, M. Bagatti, A. Ori, R. Gandolfi and M. Burdisso, *J. Chem. Soc.*, *Faraday Trans.*, 1993, **89**, 29.
9 A. Rastelli, M. Bagatti and R. Gandolfi, *J. Chem. Soc.*, *Faraday Trans.*, 1993, **89**, 3913.
10 A. Rastelli, M. Cocchi, E. Schiatti, R. Gandolfi and M. Burdisso, *J. Chem. Soc.*, *Faraday Trans.*, 1996, **86**, 783.
11 M. Freccero, R. Gandolfi, M. Sarzi-Amadé and A. Rastelli, unpublished results.
12 E. Cinquini, M. Freccero, R. Gandolfi, M. Sarzi-Amadè and A. Rastelli, *Tetrahedron*, 1997, **53**, 9279.
13 J. I. Brauman, Jr and W. C. Archie, *J. Am. Chem. Soc.*, 1972, **94**, 4262.
14 L. Mévellec, M. Evers and F. Huet, *Tetrahedron*, 1996, **52**, 15103.
15 R. A. Keppel and R. G. Bergman, *J. Am. Chem. Soc.*, 1972, **94**, 1350.
16 R. Gandolfi, M. Sarzi-Amadé, A. Rastelli, M. Bagatti and D. Montanari, *Tetrahedron Lett.*, 1996, **37**, 517.
17 A. Rastelli, M. Bagatti and R. Gandolfi, *J. Am. Chem. Soc.*, 1995, **117**, 4965.
18 R. Huisgen, in *1,3-Dipolar Cycloaddition Chemistry*, ed. A. Padwa, Wiley-Interscience, New York, 1984, vol. 1, p. 1.
19 S. Sosa, J. Andzelm, C. Lee, J. F. Blake, B. L. Chenard and T. W. Butler, *Int. J. Quantum Chem.*, 1994, **49**, 511.
20 R. Sustmann, W. Sicking and R. Huisgen, *J. Am. Chem. Soc.*, 1995, **117**, 9679.
21 See also for DFT calculations in the field of pericyclic reactions, O. Wiest and K. N. Houk, *Top. Curr. Chem.*, 1996, **183**, 1.
22 E. Schmitz, *Chem. Ber.*, 1958, **91**, 1488.
23 C. Grundmann and P. Grunanger, *The Nitrile Oxides*, Springer-Verlag, Berlin-Heidelberg, New York, 1971, p. 21.
24 A. Corsico-Coda and G. Tacconi, *Gazz. Chim. Ital.*, 1984, **114**, 131.
25 Gaussian 94, Revision E.3, M. J. Frisch, G. W. Trucks, H. B. Schlegel, P. M. W. Gill, B. G. Johnson, M. A. Robb, J. R. Cheeseman, T. Keith, G. A. Petersson, J. A. Montgomery, K. Raghavachari, M. A. Al-Laham, V. G. Zakrzewski, J. V. Ortiz, J. B. Foresman, J. Cioslowski, B. B. Stefanov, A. Nanayakkara, M. Challacombe, C. Y. Peng, P. Y. Ayala, W. Chen, M. W. Wong, J. L. Andres, E. S. Replogle, R. Gomperts, R. L. Martin, D. J. Fox, J. S. Binkley, D. J. Defrees, J. Baker, J. P. Stewart, M. Head-Gordon, C. Gonzalez and J. A. Pople, Gaussian, Inc., Pittsburgh, PA, 1995.

Paper 8/05372C